

Comparative Gene Expression Signature of Pig, Human and Mouse Induced Pluripotent Stem Cell Lines Reveals Insight into Pig Pluripotency Gene Networks

Yajun Liu · Yangyang Ma · Jeong-Yeh Yang · De Cheng ·
Xiaopeng Liu · Xiaoling Ma · Franklin D. West ·
Huayan Wang

© Springer Science+Business Media New York 2013

Abstract Reported pig induced pluripotent stem cells (piPSCs) have shown either a bFGF-dependent state with human embryonic stem cell (ESC) and mouse epiblast stem cell (EpiSC) morphology and molecular features or piPSCs exist in a LIF-dependent state and resemble fully reprogrammed mouse iPSCs. The features of authentic piPSCs and molecular events during the reprogramming are largely unknown. In this study, we assessed the transcriptome profile of multiple piPSC lines derived from different laboratories worldwide and compared to mouse and human iPSCs to

Electronic supplementary material The online version of this article (doi:10.1007/s12015-013-9485-9) contains supplementary material, which is available to authorized users.

Y. Liu · Y. Ma · D. Cheng · X. Liu · X. Ma · H. Wang
College of Veterinary Medicine, Shaanxi Center for Stem Cell
Engineering and Technology, Northwest A&F University, Yangling,
Shaanxi 712100, China

J.-Y. Yang · F. D. West
Regenerative Bioscience Center, University of Georgia,
Athens, GA, USA

J.-Y. Yang · F. D. West
Department of Animal and Dairy Science, University of Georgia,
Rhodes Center for Animal and Dairy Science, 425 River Road,
Athens, GA 30602-2771, USA

D. Cheng
Department of Cellular and Molecular Physiology, College of
Medicine, Pennsylvania State University, 500 University Drive,
Hershey, PA 17033, USA

H. Wang (✉)
Department of Animal Biotechnology, College of Veterinary
Medicine, Northwest A&F University, Yangling,
Shaanxi 712100, China
e-mail: hhwang101@163.com

H. Wang
e-mail: hhwang101@nwsuaf.edu.cn

determine the molecular signaling pathways that might play a central role in authentic piPSCs. The results demonstrated that the up-regulation of endogenous epithelial cells adhesion molecule (EpCAM) was correlated with the pluripotent state of pig pluripotent cells, which could be utilized as a marker for evaluating pig cell reprogramming. Comparison of key signaling pathways JAK-STAT, NOTCH, TGFB1, WNT and VEGF in pig, mouse and human iPSCs showed that the core transcriptional network to maintain pluripotency and self-renewal in pig were different from that in mouse, but had significant similarities to human. Pig iPSCs, which lacked expression of specific naïve state markers *KLF2/4/5* and *TBX3*, but expressed the primed state markers of *Otx2* and *Fabp7*, share defining features with human ESCs and mouse EpiSCs. The cluster of imprinted genes delineated by the delta-like homolog 1 gene and the type III iodothyronine deiodinase gene (*DLK1-DIO3*) were silenced in piPSCs as previously seen in mouse iPSCs that have limited ability to contribute to chimaeras. These key differences in naïve state gene and imprinting gene expression suggests that so far known piPSC lines may be more similar to primed state cells. The primed state of these cells may potentially explain the rare ability of piPSCs to generate chimeras and cloned offspring.

Keywords Pig · iPS cell · GeneChip · *EpCAM* ·
Gene expression profiling

Introduction

Domestic pigs are an ideal animal model for regenerative medicine due to their close resemblance to humans in body size, physical structure and metabolism. Though intense efforts have been made to establish porcine embryonic stem cells (ESCs) since the 1990s, few validated successes have

been achieved [1–3]. Since the novel development of mouse induced pluripotent stem cells (iPSCs), where somatic cells were reprogrammed into a pluripotent state by ectopic expression of defined transcription factors [4], multiple pig iPSC (piPSC) lines have been successfully established [5–8]. However, most known piPSC lines have shown differences in morphology, pluripotent markers and are maintained in a number of varying culture conditions [5, 8, 9]. Up to now only one report has shown that piPSCs are capable of producing chimeric pigs and have demonstrated germline competency of these animals [2]. In addition, our group recently reported cloned piglets from piPSCs [10]. However, the cloning rate with piPSCs was significantly lower than rates with standard somatic control cells. The difficulty to produce cloned pigs and viable chimeras using piPSCs might result from aberrant regulation of pluripotent networks that regulate self-renewal and differentiation. Further examination of gene expression signatures may aid in answering the fundamental questions regarding the pluripotent state of piPSCs.

In order to maintain the pluripotent state in murine and human pluripotent cells (ESCs and iPSC), a number of key signaling pathways and gene expression networks have been identified [11]. Transcription factors OCT4 (also known as POU5F1), SOX2 and NANOG, as well as the JAK-STAT, NOTCH, TGFB1, WNT, MAPK and VEGF signaling pathways, all have important roles in regulating and maintaining stem cell pluripotency [12]. Although human and mouse pluripotent cells show many similarities, human and mouse cells are dependent on different pathways to maintain pluripotency. Mouse pluripotent stem cells depended on the cytokines leukemia inhibitory factor (LIF) and bone morphogenetic protein 4 (BMP-4) to maintain their pluripotent state. Conversely, human ESCs depended on basic fibroblast growth factor (bFGF) and Activin A to retain pluripotency and self-renewal properties [13]. To gain insight into the global molecular signature of pluripotency a number of approaches have been used including genome-wide expression profiling utilizing expressed sequence tag (EST) analysis [14], serial analysis of gene expression (SAGE) [15], massively parallel signature sequencing (MPSS) [16] and DNA microarrays [17]. Recently, single-cell RNA sequencing revealed the transcriptome dynamics at the single cell level and showed the sequential transcriptional changes in pathways during human and mouse embryo development [18]. These studies have provided molecular signatures of pluripotent cells and preimplantation embryos and have laid a foundation to identify the pluripotent cell fate and define pig iPSC identity.

Although a wealth of information currently exists for genetic networks involved in the maintenance of pluripotency in mouse and human pluripotent stem cells, the molecular mechanisms for pluripotency in pig is poorly understood. The uniform and authentic characteristics of piPSCs have not yet been defined. In this study, we assessed the transcriptome

profile of multiple piPSC lines derived from different laboratories and compared them to pig somatic and embryonic stem cells and mouse and human iPSCs to determine the molecular signaling pathways that may play a central role in authentic piPSCs.

Materials and Methods

Cell Culture

Fetal pigs were purchased from a licensed local slaughterhouse and the protocol to work with pig specimens was based on the farm animal research guidelines approved by the Animal Research Committee of Northwest A&F University. Pig embryonic fibroblasts (PEFs) were derived from a 35-day-old fetal pig. Cells were grown in Dulbecco's Modified Eagle's Medium (DMEM, Gibco, USA) supplemented with 15 % FBS, 2 mM L-glutamine, 50 U/mL penicillin and 50 µg/mL streptomycin at 38.5 °C and in 5 % CO₂ for 72 h. The piPS cells (PS24 and 30 AC5) were maintained on mitotically inactive mouse embryonic fibroblast (MEF) feeder layers derived from ICR mice, and passaged using 1 mg/mL type IV Collagenase (Invitrogen, USA) and 0.05 % Trypsin (Invitrogen, USA) every 2 to 3 days. Other pig iPSC lines were obtained from different labs and were cultured in conditions based on previously established protocols (Table 1) [6, 9].

Alkaline Phosphatase Assay

The alkaline phosphatase (AP) activity of infected cells was detected by an alkaline phosphatase substrate AST Fast Red TR and a-Naphthol AS-MX Phosphate (Sigma Aldrich) according to the manufacturer's instructions. Briefly, cells were washed twice with phosphate-buffered saline (PBS), and then fixed with 4 % paraformaldehyde in PBS (pH 7.4) for 15 min at room temperature, followed by three washes with PBS. Cells were incubated with the mixture (Fast Red TR 1.0 mg/mL, Naphthol AS-MX 0.4 mg/mL in 0.1 M Tris buffer) at room temperature. After incubating for 10–20 min, AP positive cells became red in color. Images were documented by microscopy (Leica).

Cytogenetic Analysis

The karyotype of pig iPSCs was analyzed following the standard procedure described in Cell Biology Laboratory Manual at <http://homepages.gac.edu/~cellab/chpts/chpt10/ex10-6.html/>.

Table 1 The iPS and ES cell lines from different laboratories

Name	Pig	Pig	Pig	Pig	Pig	Mouse	Mouse	Mouse	Mouse	Human
Recipient cell	PEF	PEF	PPF	PEF	ICM	MEF1 MEF2	MEF	MEF	Epiblast	dH1f, dH1cfl6, MRC5
Pluripotent Cells	PS24, 30 AC5	iPF4-2	IC1, ID4, ID6	piPS-w	pESK	4F-iPS	Induced cells in Day 4, 8, 12, and 16	IP14D-1, IP14D-101, ES-R1	Naïve ES ES-R1	dH1f-iPS, dH1cfl6-iPS, MRC5-iPS BG01 ES HI ES
Transcription Factors Vectors	mOSKM	hOSKM	hOSKM	hOSKMNL	hKLF4/OK	mOSK	mOSKM	mOSKM	SB431542 JAK inhibitor I	hOSKM
Affymetrix Platform	retrovirus	DOX-inducible lentivirus	lentivirus	lentivirus	lentivirus	retrovirus	DOX-inducible lentivirus	retrovirus	Small-molecule treatment	retrovirus
	Pig Genome Array	Pig Genome Array	Pig Genome Array	Pig Genome Array	Pig Genome Array	Mouse Genome 430 2.0 Array	Mouse Genome 430 2.0 Array	Mouse Genome 430 2.0 Array	Agilent-014868 Whole Mouse Genome Microarray	Human Genome ui33 plus 2.0 Array
GEO Number	GSE48434	GSE48434	GSE15472	GSE48434	GSE26369	GSE15267	GSE10871	GSE21515	GSE15603	GSE9832
Reference	[7]	[6]	[5]	[9]	[19]	[20]	[21]	[22]	[23]	[24]

All of the microarray data can be retrieved through the corresponding GEO number

Immunocytochemical Analysis

For immunocytochemical analysis, cells were fixed with 4 % paraformaldehyde in PBS (pH 7.4) for 15 min at room temperature. The fixed cells were washed twice with ice-cold PBS, then incubated with PBS containing 0.1 % Triton X-100 for 10 min, and washed three times with PBS again. After blocking in BSA-blotting buffer for 30 min, cells were incubated in BSA-blotting buffer with primary antibodies in a humidified chamber for 1 h at 37 °C or overnight at 4 °C. The antibodies include anti-Nanog (1:200, Abcam #ab80892), anti-SSEA1 (1:50, Millipore #90230), anti-SSEA4 (1:50, Millipore #90231), anti-TRA-1-60 (1:50, Millipore #90232), and anti-TRA-1-81 (1:50, Millipore #90233). The negative control was conducted by incubating cells without primary antibody to eliminate nonspecific reactions. Cells were washed and stained for 1 h in secondary anti-mouse (1:200, Abcam #ab6787) or anti-rabbit (1:200, Abcam #ab6702) antibody conjugated with FITC or TRITC. For nuclear staining, fixed cells were incubated for 2 min with 10 mg/mL fluorescent dye of Hoechst33342. The images were documented on a Leica fluorescence microscope.

Microarray Analysis

The total RNAs were extracted from pig iPSC lines using RNeasy Mini Kits (QIAGEN). RNA labeling (IVT Labeling Kit, Affymetrix), hybridization with GeneChip (Affymetrix GeneChip Pig Genome Array, containing 23,937 probes, representing 20,201 genes), scanning (GeneChip Scanner 3000, Affymetrix) and quantification were conducted by CapitalBio Corporation (Beijing, China). The data were processed with the Robust Multiarray Analysis (RMA) algorithm in GeneSpring for background adjustment, normalization and log₂-transformation of perfect match values. By applying the GeneSpring normalization algorithms, the data were subjected to per chip and per gene normalization. By taking the median expression value of all probe sets on a chip and dividing each gene expression value by this median value, samples were subjected to a per chip normalization. In a second step, a transformation followed as a per gene normalization in which the median expression value of a given gene across all arrays was calculated and used to divide all gene expression values of that particular gene across all arrays. Because pig arrays are poorly annotated, the Affymetrix Pig Annotation Revision 5 (<http://www4.ncsu.edu/~stsai2/annotation/>) was used for the annotation information of pig probes [25]. Probe sets with gene-level normalized intensities greater than log (base-2.0) of 5.0 in a minimum of one sample were excluded from ANOVA. The data were then filtered based on their flag values P (present) and A (absent) to remove probe sets for which the signal intensities for all the treatment groups were in the lowest 20 percentile of all intensity values. ANOVA

incorporating the Benjamini–Hochberg FDR multiple testing correction, with a significance level of p -value < 0.05 to be performed get the differentially expressed genes between different groups. Hierarchical cluster analysis was performed to assess correlations among samples for each identified gene set with Euclidean distance and average linkage statistical methods. The principal component analysis which highlights the group of iPSCs far from the starting cell type is an unsupervised clustering and visualization approach for analyzing data derived from gene expression array. The unbiased PCA algorithm in GeneSpring was applied to all samples of pig iPSCs and fibroblasts, using all 23,937 probes on the Pig Genomechip to look for underlying cluster structures. The microarray data were deposited in GEO database, and the accession codes are: GSM1178697 for PEF; GSM1178698 for pAFSC; GSM1178699 for PS24; GSM1178700 for 30 AC5; GSM1178701 for iPF4-2; and GSM1178702 for iPSCs-w.

Database for Annotation, Visualization, and Integrated Discovery

The function of the up- or down-regulated genes in iPSCs versus somatic cells both significantly ($p < 0.001$) and numerically (± 2 -fold change) were investigated by using the Database for Annotation, Visualization and Integrated Discovery (DAVID) v6.7 [26] based on the GO annotations [27]. In addition, groups of genes associated with specific pathways, based on the Kyoto Encyclopedia of Genes and Genomes (KEGG), were analyzed together to assess pathway regulation during the reprogramming process.

Genes were grouped into specific ontology functional groups by the core analysis of Ingenuity Pathways Analysis software (IPA, www.ingenuity.com). To visualize and explore the molecular interaction networks of the differentially expressed genes between iPSCs and fibroblasts, subsequent data were uploaded into IPA to organize the differentially expressed genes into networks based on the Ingenuity Knowledge Database (IKB), an extensive, manually created database of functional direct and indirect interactions between genes from peer-reviewed publications. Networks are rated based on the probability of finding the interested genes in a given network as compared to a set of randomly selected genes. The network's score (p score) is the exponent of the P value determined using Fisher's exact test. Gene lists were analyzed and networks, pathways and lists of associated molecular functions were produced.

Oocyte in Vitro Maturation and Parthenogenesis Activation

Pig oocytes were aspirated from follicles (2–6 mm in diameter) using a 10 mL syringe with an 18 gauge needle. The oocytes matured in vitro were performed as previously

described [28]. Briefly, oocytes were matured in modified Medium 199 supplemented with 10 ng/mL epidermal growth factor, 10 IU/mL Pregnant mare's serum gonadotropin (PMSG, Sigma, USA), 10 IU/mL Human chorionic gonadotropin (hCG, Sigma, USA), 2.5 IU/mL Follicle-stimulating hormone (FSH, Sigma, USA), 1 % Insulin-transferrin-selenium (ITS, Gibco, USA) at 38.5 °C and in 5 % CO₂ and saturated humidity in air for 42 h. Oocyte maturation was determined based on the protrusion of the first polar body. To obtain parthenogenetically activated embryos, the denuded oocytes were incubated in an activation medium from Cyto Pulse Sciences Company (MA, USA) for 5 min. The oocytes were then transferred into two 0.2-mm-diameter platinum electrodes with a 1 mm gap covered with the activation medium in a chamber connected to an electrical pulsing machine (PA-4000S, Cyto Pulse Sciences). The activation was conducted with a single DC pulse of 1.5 kV/cm for 30 ms. After culturing for 3 h in TCM199 medium containing 2 mM 6-dimethylaminopurine (Sigma, USA), embryos were washed in the embryo culture medium (PZM-3 medium with 0.3 % (w/v) BSA) and cultured for 7 days at 38.5 °C and in 5 % CO₂. Blastocysts were harvested 7 days post-activation and frozen in embryo lysis buffer (5 mM Dithiothreitol, 20 U/mL RNase inhibitor, 1 % NP-40) for the preparation of RNA.

RT-PCR Analysis

Total cellular RNAs from pig fibroblasts, piPSCs and embryos were extracted using the TRIzol Reagent (Invitrogen, USA) according to the manufacturer's procedure. The RNA samples were examined by the measurement of OD_{260/280} ratio and the samples with a ratio of 2.0 were used for reverse transcription. One μ g of RNA was reverse-transcribed using the High-Capacity cDNA Reverse Transcription Kit (Applied Biosystems, USA) following manufactures instructions. Semi-quantitative RT-PCR reactions were performed for 32 cycles at 94 °C 30 s, 54 °C 30 s, and 72 °C 30 s. PCR products were confirmed by DNA sequencing and agarose gel electrophoresis. A 10-fold dilution of cDNA products was used as a template to perform qRT-PCR with SYBR Green PCR master mix. After 10 min of denaturation of cDNA template at 95 °C, the reactions were performed for 40 cycles at 95 °C 15 s, 56 °C 30 s, and 72 °C 30 s. qRT-PCR measurements were performed on three unique biological replicates and each reaction was performed in triplicate. Melting curve analysis was conducted after each cycle to confirm the specificity. The glyceraldehydes 3-phosphate dehydrogenase (*GAPDH*) was used as internal control for all reactions. The threshold cycle (C_t) formula was used to calculate changes in gene expression. Primers were designed with Primer 5.0 software and synthesized by Shengong Biotechnology Corporation (Shanghai, China). The primers used in this study are listed in Table S7.

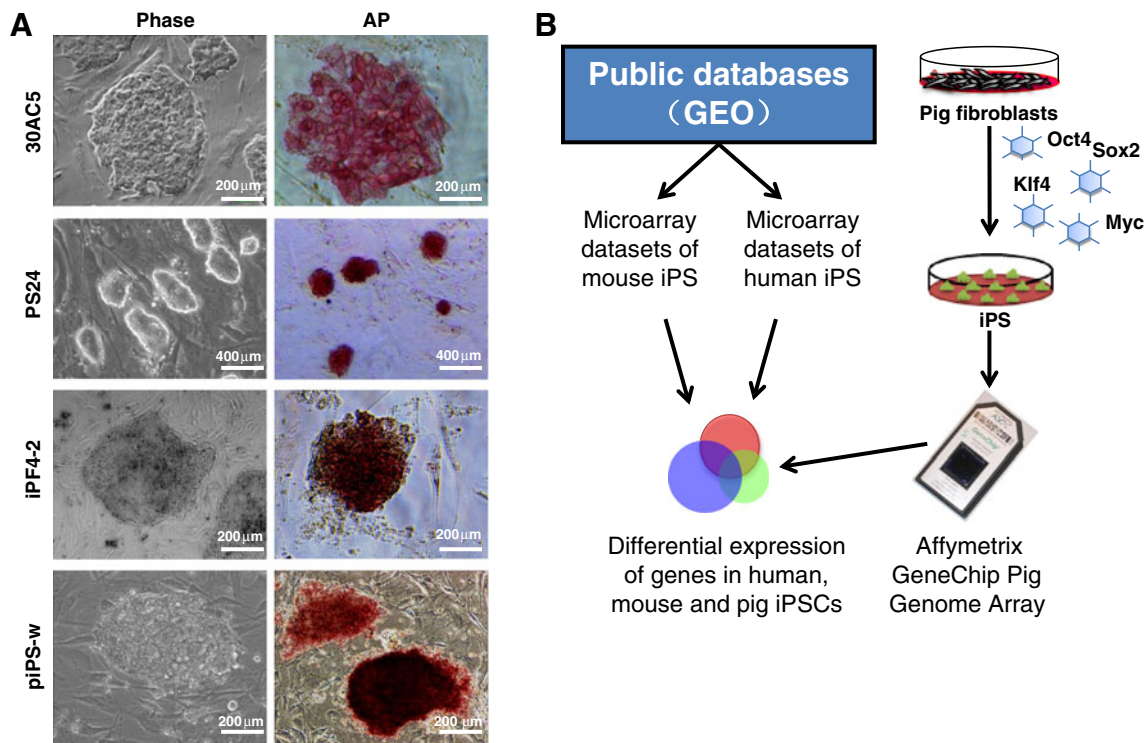


Fig. 1 Morphology of pig iPSCs derived from different labs and the description of gene signature analysis. **a** piPSCs from different laboratories showed both flattened (30 AC5, iPF4-2 and piPS-w) and dome-shaped (PS24) morphology and were positive for AP staining. **b**

Schematic of the analytical process by Affymetrix GeneChip Pig Genome Array. The microarray data of human and mouse iPSCs were acquired from GEO database

Statistical Analysis

All values are presented as mean \pm SD, unless indicated otherwise. Statistical significance was accepted at p -value $<$ 0.05 and determined using the two-tailed t -test with equal variance by SPSS 16.0.

Results

Gene Expression Profiling of piPSCs

To determine the pluripotency gene expression signature in pigs, we compared 7 unique piPSC lines, a pig embryonic stem cell (pESK) line, a pig amniotic fluid derived multipotent stem cell (pAFSC) line, a pig embryonic fibroblast (PEF) line and a pig fetal fibroblast (PFF) line. The detailed information of these lines are summarized in Table 1. The bFGF-dependent piPSC line piPS-w [9], 30 AC5 [7] and iPF4-2 [6] showed flat and compact colony morphology which are similar to human ESCs and mouse EpiSCs (Fig. 1a). The piPSC lines IC1, ID4 and ID6 reported by the Roberts' Lab also showed the flattened morphology [5]. Only the LIF-dependent piPSC line PS24 displayed the dome-shaped morphology characteristic of mouse ESCs [7]. Pig amniotic fluid derived multipotent stem cells (pAFSCs) showed

fibroblastoid morphology and retaining self-renewal capability and multi-lineage differentiation potentials as previously determined in our lab [29].

Genome-wide transcriptome profiling using the Affymetrix pig microarray (the analytical pathway is summarized in a schematic diagram; Fig. 1b) indicated that piPSC lines clustered differently from somatic cell lines, in which there were three groups: PS24 and 30 AC5 (Fig. 2a, a); piPS-w and iPF4-2 (Fig. 2a, b); and IC1, ID4 and ID6 (Fig. 2a, c). The principal component analysis (PCA) of global gene expression patterns showed transcriptome-scale similarities among piPSC lines, but highlighted global differences between piPSC lines and pAFSCs, pESKs and fibroblasts. The pAFSCs, which did not form teratoma when injected into immunodeficiency mice [29], were clustered individually, indicating that pAFSCs are multipotent stem cells and likely not pluripotent stem cells. The cell lines that retained the developmental abilities to generate cloned piglets (iPF4-2 [10]), chimera (piPS-w [9]) and rod photoreceptors (ID6 [30]) were cluster closely (Fig. 2b). The Pearson correlation analysis showed that piPS-w line retained strong transcriptome similarity with other piPS cell lines, but cell lines of PS24 and 30 AC5 had less correlation with other lines (Fig. 2c). These observations indicated that piPSC lines derived from different laboratories were reprogrammed, but possess a broad range in transcriptome profiles.

Pluripotent Markers for piPSCs

The comparative analysis of global gene expression patterns in different piPSC lines was conducted by plotting 30 AC5 (fold change >2, $p < 0.05$) and PS24 (fold change >2, $p < 0.05$) against other piPSC lines (Fig. 3a). Since *NANOG* and *SOX2* genes were not included in the Affymetrix Pig GeneChipe, we monitored the expression levels of *OCT4* and *LIN28*, which were highly expressed in lines of iPS-w, ID6 and iPF4-2 compared to 30 AC5 and PS24 lines. In addition, it was noted that *EpCAM* expression was highly upregulated in piPSC lines that retained in vivo developmental potential, but was lowly expressed in somatic cells (PEF) or piPSCs (PS24 and 30 AC5) that displayed limited in vivo developmental potential (Fig. 3b). *EpCAM* had previously been found to be highly up-regulated in mouse iPSCs (mouse microarray, GEO database, access number GSE15267, GSE10871 and GSE21515; Fig. S3C). Gene *ZFP42* (also called *REX1*) is a key landmark for pluripotent cells in human and mouse. The

pairwise scatter plots of three cell lines that were derived from the same lab showed that *ZFP42* was highly expressed in ID6 compared with IC1 and ID4 [5] (Fig. 3c). However, it was noted that only the ID6 piPSC line showed up regulation of the *ZFP42* gene. These results suggest that *EpCAM* and *ZFP42* could be suitable markers to evaluate the pluripotent state of piPSCs.

Comparative Analysis of Pathways in iPSCs

We identified 1846, 2596 and 1246 genes that were upregulated in pig, mouse and human iPSCs compared to fibroblasts (Fig. 4a). There were 253 genes that were upregulated in all three species (Table S1). Large numbers of upregulated genes were classified into the downstream targets of transcription regulators (Table S2). For instance, there are 11 upregulated genes that are regulated by Oct4. Venn diagram of upregulated genes in iPF4-2, ID6 and piPS-w cells showed that 2651,

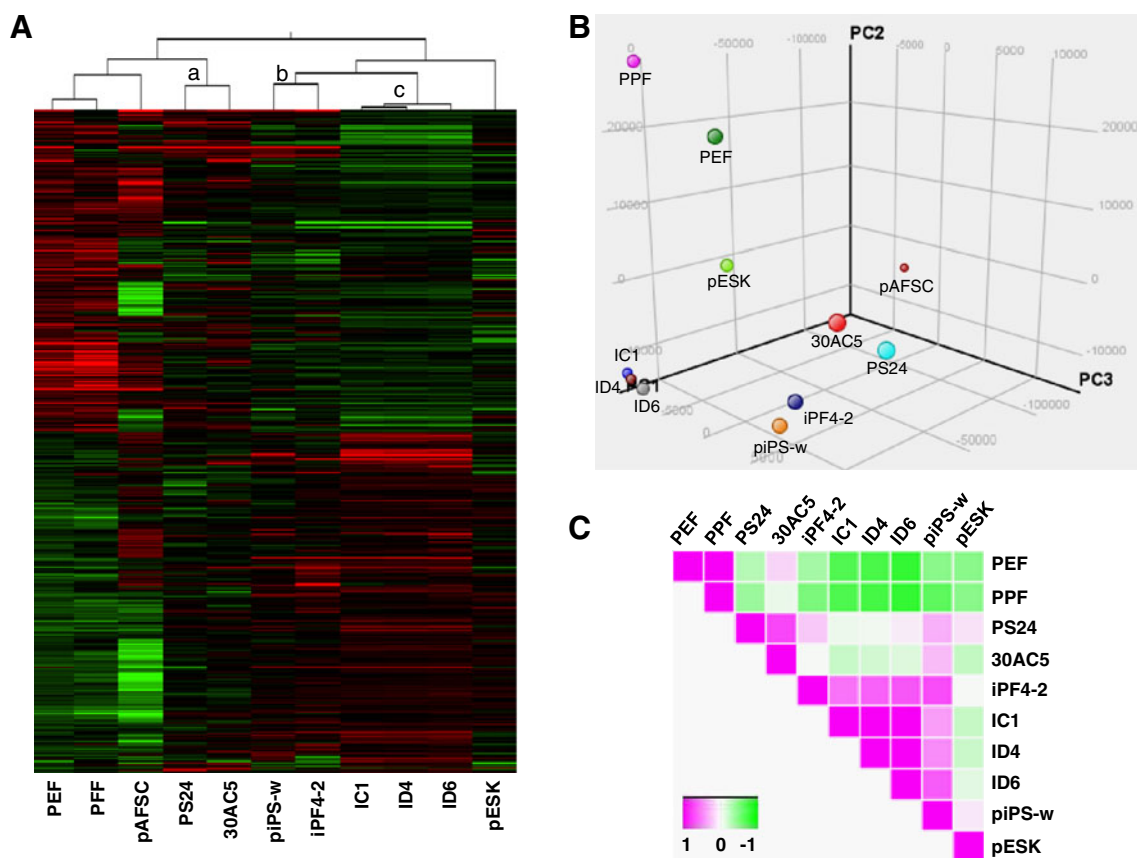


Fig. 2 Hierarchical clustering and gene expression signature of piPSCs. **a** Hierarchical clustering and heatmap of global gene expression patterns include pig embryo fibroblast (PEF), pig fetal fibroblast (PFF), pig amniotic fluid stem cell (pAFSC), pig iPSC lines PS24, 30 AC5, piPS-w, iPF4-2, IC1, ID4 and ID6, and pig ESC line pESK show significant similarities between piPSC lines. **b** Principal component analysis (PCA)

of global gene expression patterns of piPSCs, pAFSC, pESK, and fibroblasts. Values indicate the contribution of principal component 1 (PC1), 2 (PC2) and 3 (PC3), which denote the transcriptome similarities between samples. **c** Pearson correlation analysis of piPSC lines. The correlations among piPSC lines ranged from +1 to -1

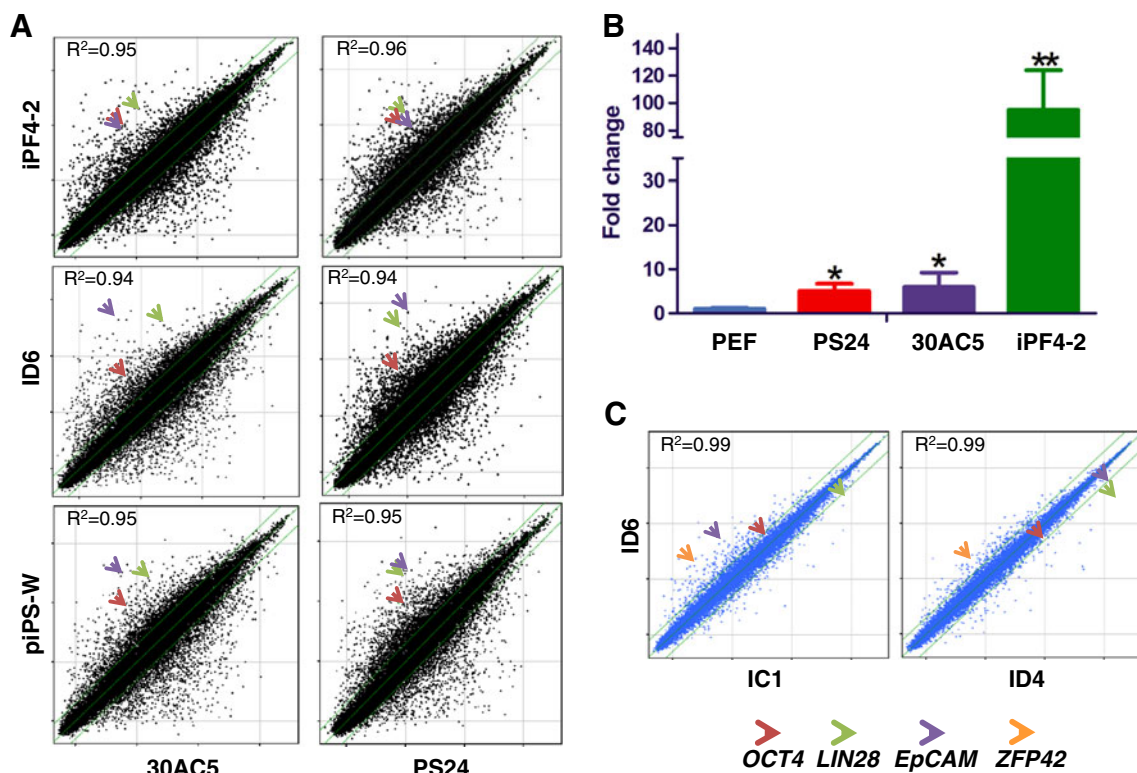


Fig. 3 Comparative analysis of global gene expression patterns in different piPSC lines. **a** Pairwise scatter plots of piPSC lines 30 AC5 and PS24 lines vs. iPF4-2, ID6 and iPS-w showed iPF4-2, ID6 and iPS-w possessed higher expression levels of *OCT4*, *LIN28* and *EpCAM*. **b** Quantitative RT-PCR analysis demonstrated higher *EpCAM* expression in iPF4-2 than piPSC lines PS24 and 30 AC5 and PEFs. mRNA levels

were normalized to GAPDH internal control. * $p < 0.05$, ** $p < 0.01$ (mean \pm SD, $n = 3$). **c** Pairwise scatter plots of IC1 and ID4 lines vs. ID6 line show *Rex1* is upregulated in ID6 compared with IC1 and ID4 [5]. Gene expression levels are depicted on log₁₀ raw intensity value; the green lines delineate the boundaries of 2-fold difference in gene expression levels; R^2 values (≤ 1) indicate similarity in global gene expression

2489 and 2942 genes were upregulated compared with fibroblast, respectively (Table S3). Of these genes, 1217 genes were commonly upregulated in all three piPSC lines (Fig. 4b). The top ten upregulated genes in piPSCs were listed in Table 2. Ingenuity network analyses of 1217 genes were performed, and identified 13 networks (Table S4). The biological relationship between genes and identified network is graphically represented. The biological function of these genes is closely associated with “cellular movement, cancer and reproductive system disease”, which contained 35 focus molecules (Fig. S2). Ingenuity pathway analysis (IPA) of the top ten significantly enriched functional pathways in iPSCs of pig, mouse and human showed that several canonical pathways including “Oct4 in Mammalian Embryonic stem cell”, “ESC Differentiation into Cardiac Lineages” and “Mouse ESC Pluripotency” were found to be highly upregulated in all three species, demonstrating that piPSCs share the core transcriptional network (Fig. 4c). However, some pathways such as “G α 12/13 signaling pathway” and “BMP signaling pathway” were dominant in piPSCs, but not in mouse and human iPSCs, while “Transcriptional Regulatory Network in ESC” and “Tight Junction Signal pathway” seen in mouse and human were not

dominant in piPSCs. This result further supported key similarities but also highlighted critical species specific differences.

We next closely examined five pluripotency signaling pathways including JAK-STAT, NOTCH, LIF, TGFB1 and WNT pathways in pig, mouse and human iPSCs. Heat map analysis of gene expression showed that none of the key components in the JAK-STAT and NOTCH pathways were active in pig and human iPSCs (Fig. 4d). Conversely, the downstream LIF signaling factors, such as Jak3, Tk2, Ptpn and Stat3, were significantly upregulated in mouse pluripotent cells. The expression levels of components in JAK-STAT and NOTCH pathways were different among piPSC lines, indicating that these cell lines were in diverse states of reprogramming. Most TGFB1 and WNT pathways genes were not upregulated in piPSCs relative to mouse and human cells, whereas, only transcription regulators of the WNT pathways Lef1 and Myc are upregulated in mouse cells. One of the notable exceptions was CTBP2, which was up regulated in pig cells (Fig. 4d). The species-specific pathways and alternative routes of signaling transduction that modulate stem cell self-renewal are different in pig compared to human and mouse.

Comparative Analysis of Pluripotent Gene Expressions in iPSCs

The comparison of the bFGF-dependent piPSC line piPS-w with human iPSCs and mouse EpiSCs [23] showed that there 147 upregulated genes that overlapped (Fig. 5a, a). This data showed limited conservation of the transcriptome between pig and human iPSCs and mouse EpiSCs. One gene of significant interest is methyl-CpG-binding domain protein 2 (*MBD2*), which blocks the complete reprogramming of human somatic cells to iPSCs [31], which was not silenced in piPCs. This

suggests that this gene may have inhibited the complete reprogramming of piPSCs. The EpiSC markers *Otx2* and *Fabp7*, genes expressed in mouse EpiSCs and play a role in fatty acid uptake, transport and metabolism, were also significantly upregulated in piPSCs (Table S5). The expressions of *Otx2* and *Fabp7* were confirmed by microarray and qRT-PCR (Fig. 5b, c). We also compared the LIF-dependent piPSC line PS24 with human iPSCs and mouse ESCs. There were only 42 upregulated genes that overlapped among these three cell populations (Fig. 5a, b; Table S6). On the other hand, three Krüppel-like factor (Klf) family genes were upregulated in

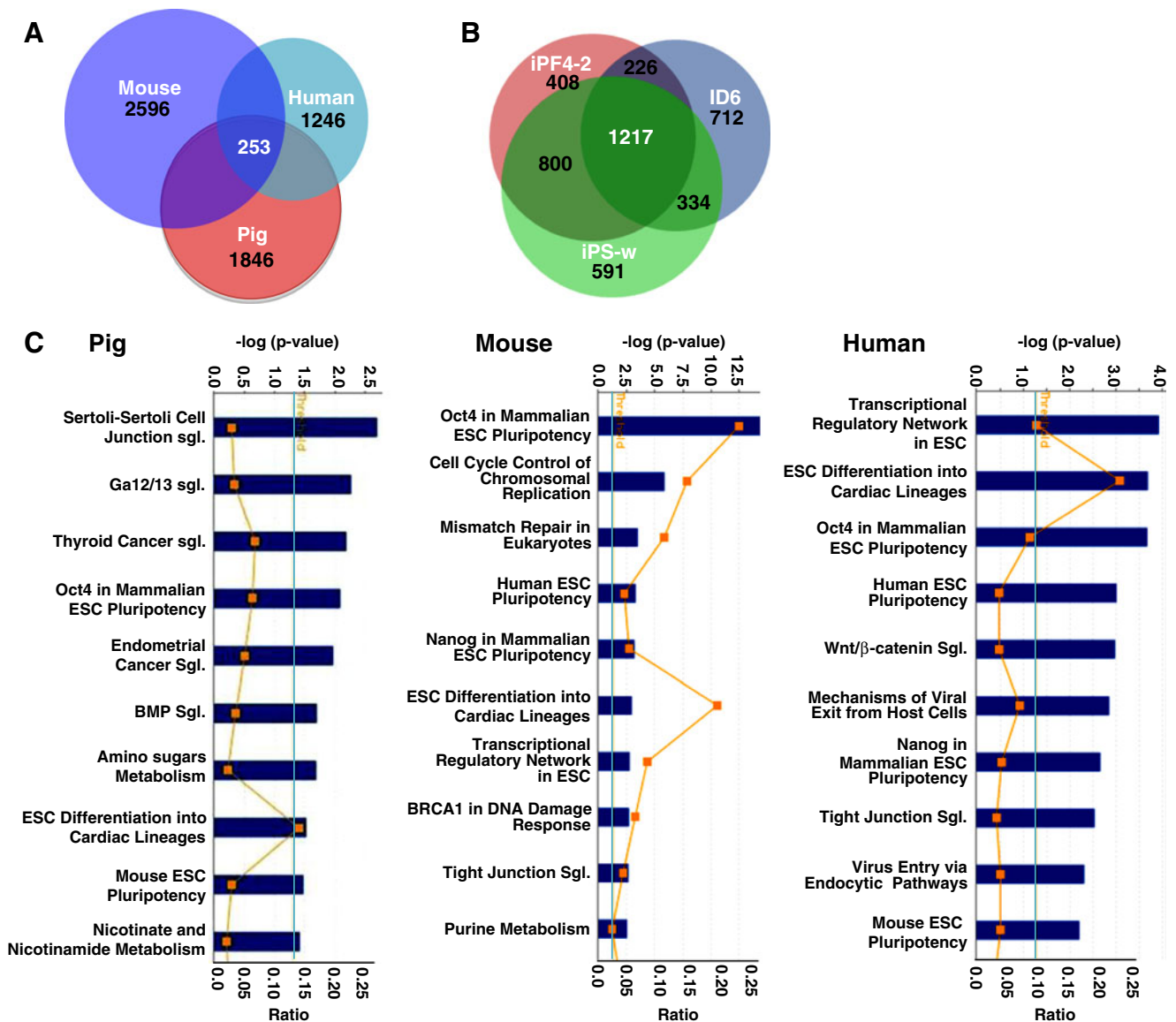


Fig. 4 Comparative analysis of pathways in different species. **a** Venn Diagram of up-regulated genes in iPSCs derived from pig, mouse, and human. **b** Venn Diagram of up-regulated genes in iPF4-2, ID6, and piPS-w cells. **c** Ingenuity Pathway Analysis of top ten significantly enriched functional pathways in iPSCs of pig, mouse, and human. *Columns* represent the p-value in logarithmic scale for each pathway. *Blue line*

indicates the significant threshold. Ratio (*orange line*) indicates the percentage of genes from the pathway vs. the total number of genes assigned to that pathway. **d** Heatmaps of genes with given roles in five signaling pathways in pig (*left*), mouse (*center*), and human (*right*). The signal values of up-regulation (*red*) and down-regulation (*green*) range from 2 to -2 folds

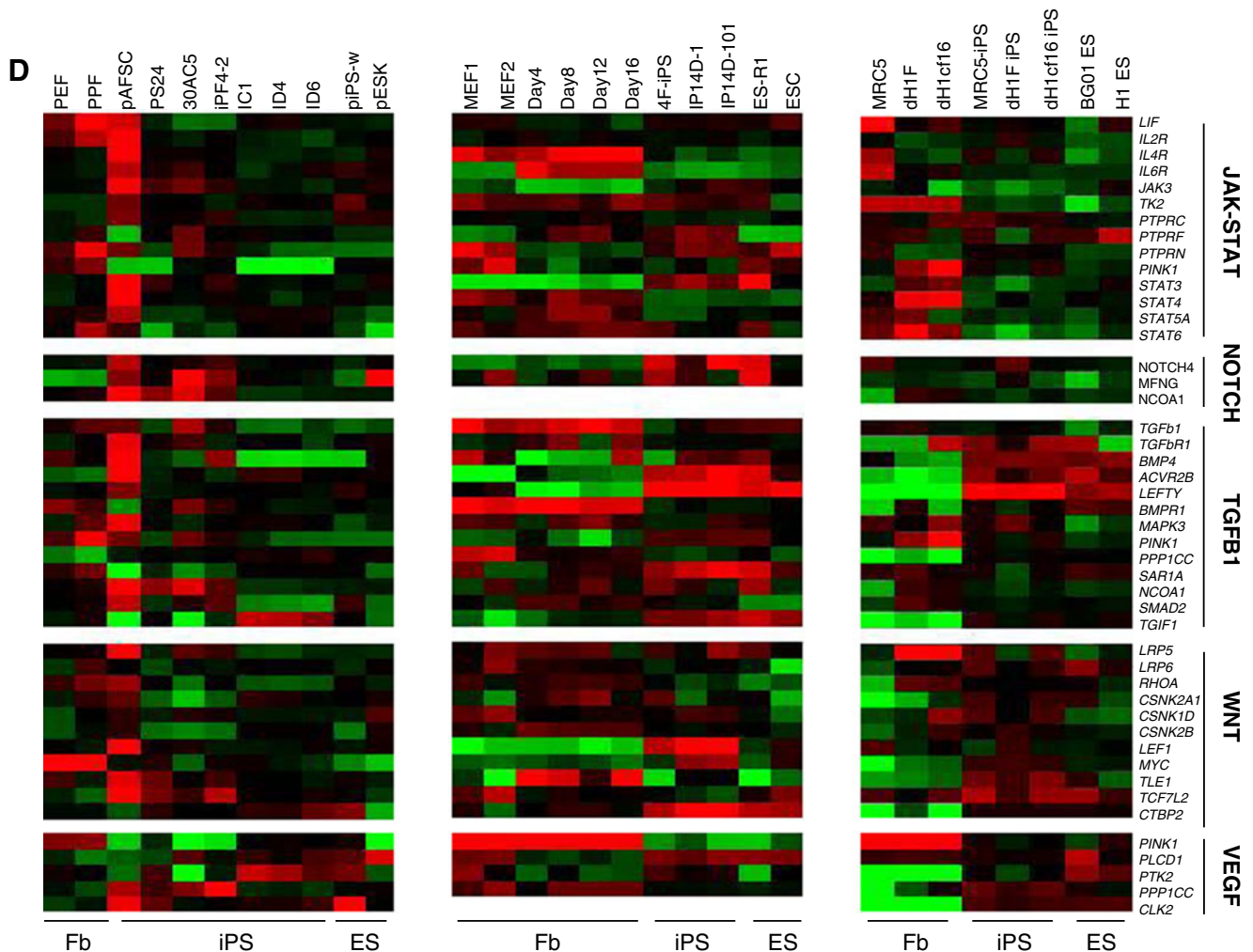


Fig. 4 (continued)

mouse iPS and ES cells, but not coordinately upregulated in pig and human iPSCs (Fig. 5b, c). The analysis of Hanna J' data [23] also showed that *KLF2/4/5* highly expressed in

Table 2 Top ten upregulated genes in piPSCs

Probe Set ID	Fold Change			Gene Symbol
	ID6	iPF4-2	piPS-w	
Ssc.24982.1.S1_at	219.7	178.1	13.1	FABP7
Ssc.9272.1.S1_at	205.0	35.4	123.7	EpCAM
Ssc.7538.1.S1_at	156.0	58.2	178.8	CDH1
Ssc.22207.1.A1_at	112.7	139.6	115.9	MAP2K1
Ssc.14081.1.A1_at	111.6	177.3	413.7	C1orf59
Ssc.24382.1.S1_at	108.4	78.5	35.6	TMEM163
Ssc.16718.1.A1_at	88.3	36.7	27.1	CTBS
Ssc.23959.1.S1_at	86.6	73.4	90.1	NFE2L3
Ssc.26067.1.S1_at	85.1	64.0	37.5	PODXL
Ssc.8004.1.A1_at	81.3	44.9	4.2	SLC16A12

mouse naïve type ESCs, but downregulated in EpiSCs (Fig. 5b, middle panel). Further investigation may be needed to reveal the core regulatory module of *KLF2/4/5* transcription factors in pig pluripotent cells. We also noted that the *Tbx3* gene that has been shown to significantly improve the quality of iPSCs was upregulated in mouse pluripotent cells, but not in pig and human cells (Fig. 5b).

TROP2 is the tumor-associated calcium signal transducer gene (also called *TACSTD2*) and is expressed in immature stem/progenitor-like cells with high levels of plasticity [32]. We determined that the *TROP2* gene was upregulated more than five folds in piPSCs, but not in any of the human and mouse cells tested (Fig. 5b, c). Semi-quantitative RT-PCR analysis also confirmed the expression of *TROP2* as well as OCT4 in pig oocyte and parthenogenetic embryo (Fig. 5d).

The microRNAs miR302/367 cluster that is located in intron 8 of *LARP7* genome is far less abundant in mESCs than in hESCs, and is also highly upregulated in mouse EpiSCs rather than in mESCs. This suggests that miR302/367 is differentially expressed between ESCs and EpiSCs

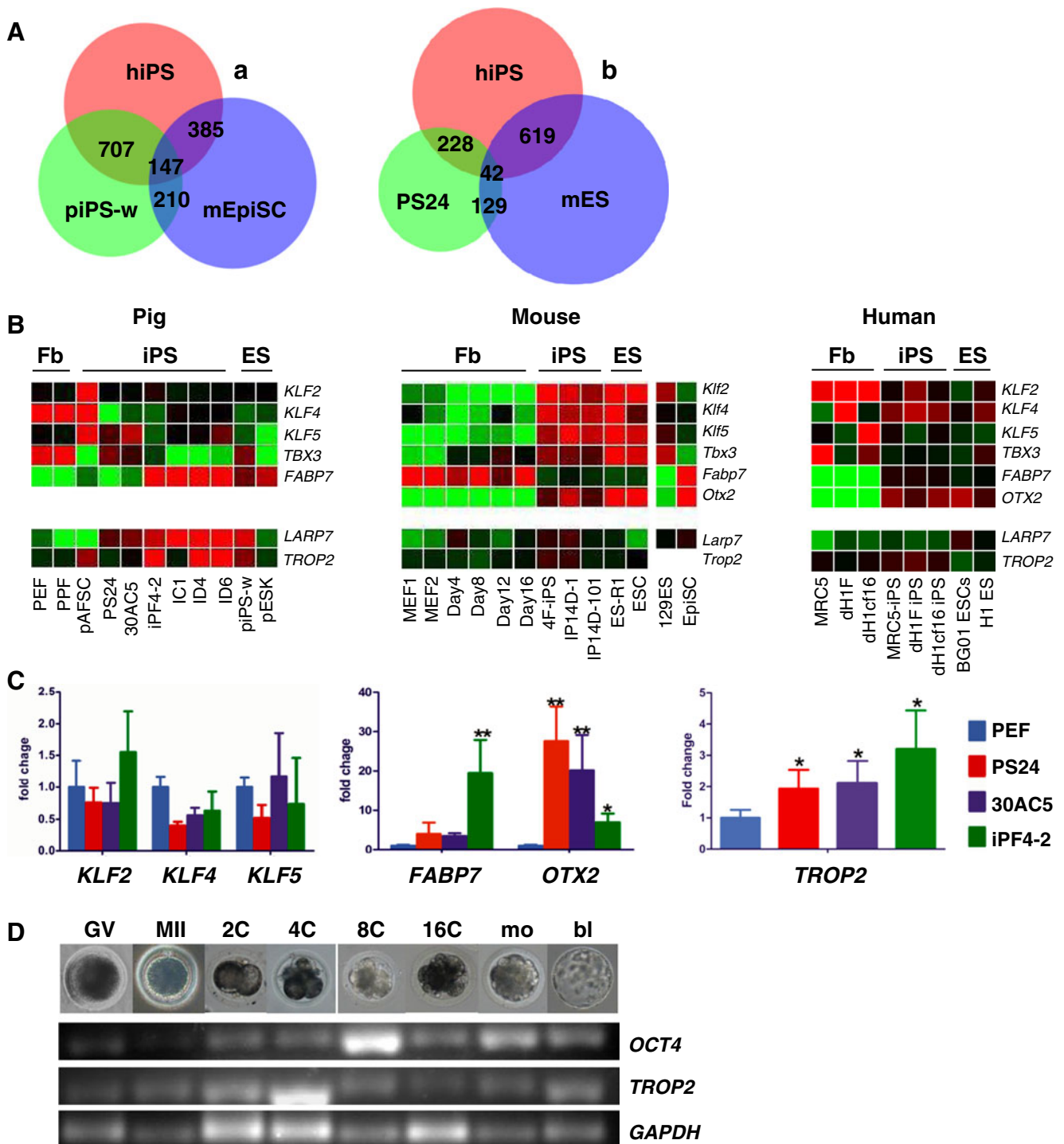


Fig. 5 Gene expression profiles of pig, mouse and human pluripotent cells. **a** Venn Diagrams show up-regulated genes in piPS-w cells vs. human iPS cells and mEpiSC cells (*a*), and in PS24 vs. human iPS cells and mES cells (*b*). **b** Heatmaps of selected genes expressed in fibroblast (Fb), iPS, EpiSC (Epi) and ES cells. Day/4, Day/8, Day/12, and Day/16 indicate the cell reprogramming date during mouse iPSC induction [21]. The signal values of up-regulation (*red*) and down-regulation (*green*) range from 2 to -2 folds. **c** Quantitative RT-PCR analysis of pluripotent

markers of *KLF2*, *KLF4*, *KLF5*, *FABP7*, *OTX2*, and *TROP2* in piPSCs. mRNA levels were normalized by internal control *GAPDH*. * $p < 0.05$, ** $p < 0.01$ (mean \pm SD, $n = 3$). **d** Semi-quantitative RT-PCR analysis showed the expressions of *OCT4* and *TROP2* in pig oocytes and parthenogenetic pre-implantation embryos. *GAPDH* was used as internal control. *GV* Germinal vesicle stage oocyte, *MI* Metaphase II stage oocyte, *mo* morula, *bl* blastocyst

[33, 34]. Two probes of Ssc.21436.2.S1 and Ssc.21436.3.A1 for Affymetrix Pig Genechip Microarray are located in exon

4–5 and exon 6–7 of *LARP7* gene (Fig. 6a). We found that *LARP7* gene was strongly upregulated in piPSCs compared

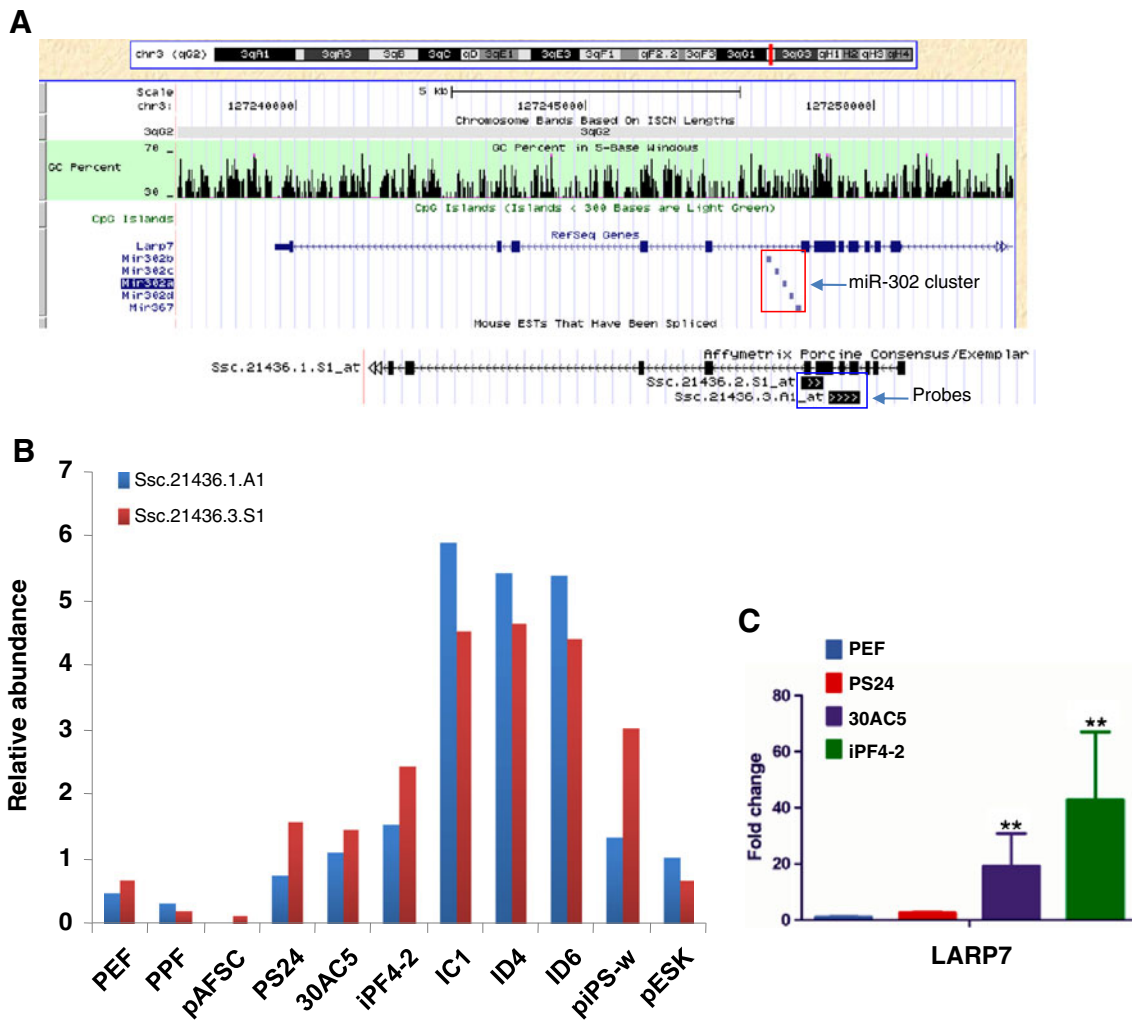


Fig. 6 Signal value of *LARP7* gene in piPSCs. **a** The locations of miR-302 cluster in red box and two *LARP7* probes of Ssc.21436.1.A1 and Ssc.21436.3.S1 in blue boxes are indicated in pig genome. **b** Affymetrix Pig Genome Array analysis of *LARP7* gene expression in piPSCs. **c**

Quantitative RT-PCR analysis showed significant up-regulation of *LARP7* gene expression in 30 AC5 and iPF4-2 piPSCs relative to PEF. ** $p < 0.01$ (mean \pm SD, $n = 3$)

with other animal species and somatic cells (Figs. 5b and 6b). The quantitative RT-PCR analysis had confirmed the increasing expression of *LARP7* in 30 AC5 and iPF4-2 cells (Fig. 6c). These results indicated that miR302/367 cluster and *LARP7* might have functional coordination or regulatory interaction in pig pluripotent cells. Further evidence of parallel transcription will be required to test this phenomenon on a larger scale.

Aberrant Silencing of Imprinted Genes in piPSCs

Imprinted genes are epigenetically regulated and expressed only from the maternally or paternally inherited chromosome. Differences in expression of imprinted genes have been directly linked to changes in developmental plasticity. For example, the cluster of *DLK1-DIO3* imprinted domain is located on distal regions of pig chromosome 7, human chromosome

14 and mouse chromosome 12, and its emergence is associated with the evolution of the placenta [34]. A recent study showed that imprinted *DLK1-DIO3* gene domain was aberrantly silenced in most mouse iPSC lines with limited developmental potential [35]. In our study, the expression level of maternal imprinted gene *GTL2* in pig iPSCs was strongly down regulated comparing with original somatic cells, while the expression of paternal imprinted gene *DIO3* was not significantly different after reprogramming (Fig. 7a). The real-time RT-PCR results confirmed *GTL2* gene silencing (Fig. 7c). Furthermore, we analyzed an additional 16 maternal imprinted and 3 paternal imprinted genes. Most tested maternal imprinted genes were down regulated in piPSCs including those cell lines that were reported to have the ability to generate chimera and cloned pigs, while the expression levels of 3 paternal imprinted genes were unchanged (Fig. 7b). We previously demonstrated that the aberrant silencing of *DLK1-*

Our study indicates that differences in pluripotency pathways likely exist between species. The top ten significantly enriched functional pathways in piPSCs varied from that in human and mouse cells. However several signaling pathway components likely play key roles in piPSC growth and differentiation including the Ga12/13 and BMP signaling pathways. In mouse pluripotent cells, the LIF signaling pathway is integrated into the core regulatory circuitry of pluripotency via two parallel pathways: Jak-Stat3 and PI3K-Akt [46]. Although the conditions that support the naïve state in pigs are not well known, we have shown in a previous report that piPSCs are unable to maintain self-renewal soon after LIF withdrawal [7]. The current transcriptome data further confirmed that the Jak-Stat3 signaling pathways were not fully activated in piPSCs using multiple unique lines. Promotion of LIF and bFGF signaling pathways could be conducive to that maintain piPSCs self-renewal. Inhibition of MEK signaling combined with GSK3 β inhibition and LIF supplementation was used to modulate pluripotency in piPSCs and segregation of pig epiblasts [47]. Elucidation of mechanisms governing pluripotent pathways in the pig would deepen our fundamental understanding of early embryogenesis and germline development, and could help to identify conditions adequate to support self-renewal requirements in ungulate species.

Altering dosage of imprinted genes is critically important for a number of developmental factors including prenatal growth, postnatal metabolism, and neurodevelopment [48]. The results of aberrant silencing of *DLK1-DIO3* domain in piPSCs are a likely explanation of the rare successful birth of chimeric offspring and limited ability to generate cloned animals from piPSCs. Loss of *DLK1-DIO3* imprinting could potentially be corrected by using serum replacement (SR) medium instead of fetal bovine serum (FBS)-containing medium [49], and supplementation with ascorbic acid as previously demonstrated [50].

In conclusion, utilizing a comparative gene expression approach between piPSCs and human and mouse iPSCs, we identified a unique pig pluripotent gene expression signature and common elements within species. We identified key markers and pathways that could serve as molecular markers and were important for maintaining piPSCs. The transcriptome of pig iPSCs will add insight to the core regulatory network of mammalian iPSCs and facilitate investigation on “stemness” in pig cells and core molecular components shared with mouse and human cells [51–54].

Acknowledgments We thank Dr. X. Lei (College of Animal Sciences, Zhejiang University, Hangzhou, China) for providing us pig iPSC cell line iPF4-2. We also thank Dr. M. Roberts for allowing us to process the data from their lab. We thank S. Zhang, M. Qing and Y. Gao for their technical supports and comments. This work was supported by the National Basic Research Program of China (2011CBA01002) and the National Natural Science Foundation of China (No.31371505).

Conflict of Interest The authors indicate no potential conflicts of interest. The authors have received research grants from the National Basic Research Program of China (2011CBA01002) and the National Natural Science Foundation of China (No.31371505).

References

- Vassiliev, I., Vassilieva, S., Truong, K. P., Beebe, L. F., McIlfrack, S. M., Harrison, S. J., & Nottle, M. B. (2011). Isolation and in vitro characterization of putative porcine embryonic stem cells from cloned embryos treated with trichostatin A. *Cellular Reprogramming*, 13(3), 205–213.
- West, F. D., Uhl, E. W., Liu, Y., Stowe, H., Lu, Y., Yu, P., Gallegos-Cardenas, A., Pratt, S. L., & Stice, S. L. (2011). Brief report: chimeric pigs produced from induced pluripotent stem cells demonstrate germline transmission and no evidence of tumor formation in young pigs. *Stem Cells*, 10, 1640–1643.
- Fujishiro, S. H., Nakano, K., Mizukami, Y., Azami, T., Arai, Y., Matsunari, H., Ishino, R., Nishimura, T., Watanabe, M., Abe, T., Furukawa, Y., Umeyama, K., Yamanaka, S., Ema, M., Nagashima, H., & Hanazono, Y. (2013). Generation of naive-like porcine-induced pluripotent stem cells capable of contributing to embryonic and fetal development. *Stem Cells and Development*, 22(3), 473–482.
- Takahashi, K., & Yamanaka, S. (2006). Induction of pluripotent stem cells from mouse embryonic and adult fibroblast cultures by defined factors. *Cell*, 126, 663–676.
- Ezashi, T., Telugu, B. P., Alexenko, A. P., Sachdev, S., Sinha, S., & Roberts, R. M. (2009). Derivation of induced pluripotent stem cells from pig somatic cells. *Proceedings of the National Academy of Sciences of the United States of America*, 106, 10993–10998.
- Wu, Z., Chen, J., Ren, J., Bao, L., Liao, J., Cui, C., Rao, L., Li, H., Gu, Y., Dai, H., et al. (2009). Generation of pig induced pluripotent stem cells with a drug-inducible system. *Journal of Molecular Cell Biology*, 1, 46–54.
- Cheng, D., Guo, Y., Li, Z., Liu, Y., Gao, X., Gao, Y., Cheng, X., Hu, J., & Wang, H. (2012). Porcine induced pluripotent stem cells require LIF and maintain their developmental potential in early stage of embryos. *PLoS One*, 7, e51778.
- Esteban, M. A., Xu, J., Yang, J., Peng, M., Qin, D., Li, W., Jiang, Z., Chen, J., Deng, K., Zhong, M., et al. (2009). Generation of induced pluripotent stem cell lines from Tibetan miniature pig. *Journal of Biological Chemistry*, 284, 17634–17640.
- West, F. D., Terlow, S. L., Kwon, D. J., Mumaw, J. L., Dhara, S. K., Hasneen, K., Dobrinsky, J. R., & Stice, S. L. (2010). Porcine induced pluripotent stem cells produce chimeric offspring. *Stem Cells and Development*, 19, 1211–1220.
- Fan, N., Chen, J., Shang, Z., Dou, H., Ji, G., Zou, Q., Wu, L., He, L., Wang, F., Liu, K., et al. (2013). Piglets cloned from induced pluripotent stem cells. *Cell Research*, 23, 162–166.
- Chen, X., Xu, H., Yuan, P., Fang, F., Huss, M., Vega, V. B., Wong, E., Orlov, Y. L., Zhang, W., Jiang, J., et al. (2008). Integration of external signaling pathways with the core transcriptional network in embryonic stem cells. *Cell*, 133, 1106–1117.
- Smith, A. G. (2001). Embryo-derived stem cells: of mice and men. *Annual review of cell and developmental biology*, 17, 435–462.
- Boyer, L. A., Lee, T. I., Cole, M. F., Johnstone, S. E., Levine, S. S., Zucker, J. P., Guenther, M. G., Kumar, R. M., Murray, H. L., Jenner, R. G., et al. (2005). Core transcriptional regulatory circuitry in human embryonic stem cells. *Cell*, 122, 947–956.
- Wei, C. L., Miura, T., Robson, P., Lim, S. K., Xu, X. Q., Lee, M. Y., Gupta, S., Stanton, L., Luo, Y., Schmitt, J., et al. (2005). Transcriptome profiling of human and murine ESCs identifies

- divergent paths required to maintain the stem cell state. *Stem Cells*, 23, 166–185.
15. Richards, M., Tan, S. P., Tan, J. H., Chan, W. K., & Bongso, A. (2004). The transcriptome profile of human embryonic stem cells as defined by SAGE. *Stem Cells*, 22, 51–64.
 16. Brandenberger, R., Khrebtkova, I., Thies, R. S., Miura, T., Jingli, C., Puri, R., Vasicek, T., Lebkowski, J., & Rao, M. (2004). MPSS profiling of human embryonic stem cells. *BMC Developmental Biology*, 4, 10.
 17. Brandenberger, R., Wei, H., Zhang, S., Lei, S., Murage, J., Fisk, G. J., Li, Y., Xu, C., Fang, R., Guegler, K., et al. (2004). Transcriptome characterization elucidates signaling networks that control human ES cell growth and differentiation. *Nature Biotechnology*, 22, 707–716.
 18. Xue, Z., Huang, K., Cai, C., Cai, L., Jiang, C. Y., Feng, Y., Liu, Z., Zeng, Q., Cheng, L., Sun, Y. E., et al. (2013). Genetic programs in human and mouse early embryos revealed by single-cell RNA sequencing. *Nature*. doi:10.1038/nature12364.
 19. Telugu, B. P., Ezashi, T., Sinha, S., Alexenko, A. P., Spate, L., Prather, R. S., & Roberts, R. M. (2011). Leukemia inhibitory factor (LIF)-dependent, pluripotent stem cells established from inner cell mass of porcine embryos. *Journal of Biological Chemistry*, 286, 28948–28953.
 20. Chen, J., Liu, J., Yang, J., Chen, Y., Ni, S., Song, H., Zeng, L., Ding, K., & Pei, D. (2011). BMPs functionally replace Klf4 and support efficient reprogramming of mouse fibroblasts by Oct4 alone. *Cell Research*, 21, 205–212.
 21. Mikkelsen, T. S., Hanna, J., Zhang, X., Ku, M., Wernig, M., Schorderet, P., Bernstein, B. E., Jaenisch, R., Lander, E. S., & Meissner, A. (2008). Dissecting direct reprogramming through integrative genomic analysis. *Nature*, 454, 49–55.
 22. Liu, L., Luo, G. Z., Yang, W., Zhao, X., Zheng, Q., Lv, Z., Li, W., Wu, H. J., Wang, L., Wang, X. J., et al. (2010). Activation of the imprinted Dlk1-Dio3 region correlates with pluripotency levels of mouse stem cells. *Journal of Biological Chemistry*, 285, 19483–19490.
 23. Hanna, J., Markoulaki, S., Mitalipova, M., Cheng, A. W., Cassady, J. P., Staerk, J., Carey, B. W., Lengner, C. J., Foreman, R., Love, J., et al. (2009). Metastable pluripotent states in NOD-mouse-derived ESCs. *Cell Stem Cell*, 4, 513–524.
 24. Warren, L., Manos, P. D., Ahfeldt, T., Loh, Y. H., Li, H., Lau, F., Ebina, W., Mandal, P. K., Smith, Z. D., Meissner, A., et al. (2010). Highly efficient reprogramming to pluripotency and directed differentiation of human cells with synthetic modified mRNA. *Cell Stem Cell*, 7, 618–630.
 25. Tsai, S., Cassady, J. P., Freking, B. A., Nonneman, D. J., Rohrer, G. A., & Piedrahita, J. A. (2006). Annotation of the Affymetrix porcine genome microarray. *Animal Genetics*, 37, 423–424.
 26. da Huang, W., Sherman, B. T., & Lempicki, R. A. (2009). Systematic and integrative analysis of large gene lists using DAVID bioinformatics resources. *Nature Protocols*, 4, 44–57.
 27. Ashburner, M., Ball, C. A., Blake, J. A., Botstein, D., Butler, H., Cherry, J. M., Davis, A. P., Dolinski, K., Dwight, S. S., Eppig, J. T., et al. (2000). Gene ontology: tool for the unification of biology. The gene ontology consortium. *Nature Genetics*, 25, 25–29.
 28. Hu, J., Cheng, D., Gao, X., Bao, J., Ma, X., & Wang, H. (2012). Vitamin C enhances the in vitro development of porcine pre-implantation embryos by reducing oxidative stress. *Reproduction in Domestic Animals*, 47(6), 873–879.
 29. Chen, J., Lu, Z., Cheng, D., Peng, S., & Wang, H. (2011). Isolation and characterization of porcine amniotic fluid-derived multipotent stem cells. *PLoS One*, 6, e19964.
 30. Zhou, L., Wang, W., Liu, Y., de Castro, J. F., Ezashi, T., Telugu, B. P., Roberts, R. M., Kaplan, H. J., & Dean, D. C. (2011). Differentiation of induced pluripotent stem cells of Swine into rod photoreceptors and their integration into the retina. *Stem Cells*, 29, 972–980.
 31. Lee, M. R., Prasain, N., Chae, H. D., Kim, Y. J., Mantel, C., Yoder, M. C., & Broxmeyer, H. E. (2013). Epigenetic regulation of NANOG by miR-302 cluster-MBD2 completes induced pluripotent stem cell reprogramming. *Stem Cells*, 31, 666–681.
 32. Stoyanova, T., Goldstein, A. S., Cai, H., Drake, J. M., Huang, J., & Witte, O. N. (2012). Regulated proteolysis of Trop2 drives epithelial hyperplasia and stem cell self-renewal via β -catenin signaling. *Genes and Development*, 26(20), 2271–2285.
 33. Jouneau, A., Ciaudo, C., Sismeiro, O., Brochard, V., Jouneau, L., Vandormael-Pourmin, S., Coppee, J. Y., Zhou, Q., Heard, E., Antoniewski, C., et al. (2012). Naive and primed murine pluripotent stem cells have distinct miRNA expression profiles. *RNA*, 18, 253–264.
 34. Stadler, B., Ivanovska, I., Mehta, K., Song, S., Nelson, A., Tan, Y., Mathieu, J., Darby, C., Blau, C. A., Ware, C., et al. (2010). Characterization of microRNAs involved in embryonic stem cell states. *Stem Cells and Development*, 19, 935–950.
 35. Stadtfeld, M., Apostolou, E., Akutsu, H., Fukuda, A., Follett, P., Natesan, S., Kono, T., Shioda, T., & Hochedlinger, K. (2010). Aberrant silencing of imprinted genes on chromosome 12qF1 in mouse induced pluripotent stem cells. *Nature*, 465, 175–181.
 36. Cheng, D., Li, Z., Liu, Y., Gao, Y., & Wang, H. (2012). Kinetic analysis of porcine fibroblast reprogramming toward pluripotency by defined factors. *Cellular Reprogramming*, 14, 312–323.
 37. Lu, T. Y., Lu, R. M., Liao, M. Y., Yu, J., Chung, C. H., Kao, C. F., & Wu, H. C. (2010). Epithelial cell adhesion molecule regulation is associated with the maintenance of the undifferentiated phenotype of human embryonic stem cells. *Journal of Biological Chemistry*, 285, 8719–8732.
 38. Chen, H. F., Chuang, C. Y., Lee, W. C., Huang, H. P., Wu, H. C., Ho, H. N., Chen, Y. J., & Kuo, H. C. (2011). Surface marker epithelial cell adhesion molecule and E-cadherin facilitate the identification and selection of induced pluripotent stem cells. *Stem Cell Reviews*, 7, 722–735.
 39. Polo, J. M., Anderssen, E., Walsh, R. M., Schwarz, B. A., Nefzger, C. M., Lim, S. M., Borkent, M., Apostolou, E., Alaei, S., Cloutier, J., et al. (2012). A molecular roadmap of reprogramming somatic cells into iPS cells. *Cell*, 151, 1617–1632.
 40. McConnell, B. B., Ghaleb, A. M., Nandan, M. O., & Yang, V. W. (2007). The diverse functions of Kruppel-like factors 4 and 5 in epithelial biology and pathobiology. *Bioessays*, 29, 549–557.
 41. Guo, G., Yang, J., Nichols, J., Hall, J. S., Eyres, I., Mansfield, W., & Smith, A. (2009). Klf4 reverts developmentally programmed restriction of ground state pluripotency. *Development*, 136, 1063–1069.
 42. Han, J. Y., Yuan, P., Yang, H., Zhang, J. Q., Soh, B. S., Li, P., Lim, S. L., Cao, S. Y., Tay, J. L., Orlov, Y. L., et al. (2010). Tbx3 improves the germ-line competency of induced pluripotent stem cells. *Nature*, 463, 1096–1100.
 43. Acampora, D., Di Giovannantonio, L. G., & Simeone, A. (2012). Otx2 is an intrinsic determinant of the embryonic stem cell state and is required for transition to a stable epiblast stem cell condition. *Development*, 140(1), 43–55.
 44. Rais, Y., Zviran, A., Geula, S., Gafni, O., Chomsky, E., Viukov, S., Mansour, A. A., Caspi, I., Krupalnik, V., Zerbib, M., et al. (2013). Deterministic direct reprogramming of somatic cells to pluripotency. *Nature*, 502, 65–70.
 45. Gafni, O., Weinberger, L., Mansour, A. A., Manor, Y. S., Chomsky, E., Ben-Yosef, D., Kalma, Y., Viukov, S., Maza, I., Zviran, A., et al. (2013). Derivation of novel human ground state naive pluripotent stem cells. *Nature*. doi:10.1038/nature12745.
 46. Niwa, H., Ogawa, K., Shimosato, D., & Adachi, K. (2009). A parallel circuit of LIF signalling pathways maintains pluripotency of mouse ES cells. *Nature*, 460, 118–122.
 47. Rodriguez, A., Allegrucci, C., & Alberio, R. (2012). Modulation of pluripotency in the porcine embryo and iPS cells. *PLoS One*, 7, e49079.

48. Da Rocha, S. T., Edwards, C. A., Ito, M., Ogata, T., & Ferguson-Smith, A. C. (2008). Genomic imprinting at the mammalian Dlk1-Dio3 domain. *Trends in Genetics*, *24*, 306–316.
49. Chen, J., Liu, H., Liu, J., Qi, J., Wei, B., Yang, J., Liang, H., Chen, Y., Wu, Y., Guo, L., et al. (2013). H3K9 methylation is a barrier during somatic cell reprogramming into iPSCs. *Nature Genetics*, *45*, 34–42.
50. Stadtfeld, M., Apostolou, E., Ferrari, F., Choi, J., Walsh, R. M., Chen, T., Ooi, S. S., Kim, S. Y., Bestor, T. H., Shioda, T., et al. (2012). Ascorbic acid prevents loss of Dlk1-Dio3 imprinting and facilitates generation of all-iPS cell mice from terminally differentiated B cells. *Nature Genetics*, *44*, 398–405.
51. Edwards, C. A., Mungall, A. J., Matthews, L., Ryder, E., Gray, D. J., Pask, A. J., Shaw, G., Graves, J. A., Rogers, J., Consortium, S., et al. (2008). The evolution of the DLK1-DIO3 imprinted domain in mammals. *PLoS Biology*, *6*, e135.
52. Esmailpour, T., & Huang, T. (2012). TBX3 promotes human embryonic stem cell proliferation and neuroepithelial differentiation in a differentiation stage-dependent manner. *Stem Cells*, *30*, 2152–2163.
53. Wang, J., Gu, Q., Hao, J., Jia, Y., Xue, B., Jin, H., Ma, J., Wei, R., Hai, T., Kong, Q., et al. (2013). Tbx3 and Nr5alpha2 play important roles in pig pluripotent stem cells. *Stem Cell Reviews*, *9*(5), 700–708.
54. Hanna, J., Cheng, A. W., Saha, K., Kim, J., Lengner, C. J., Soldner, F., Cassady, J. P., Muffat, J., Carey, B. W., & Jaenisch, R. (2010). Human embryonic stem cells with biological and epigenetic characteristics similar to those of mouse ESCs. *Proceedings of the National Academy of Sciences of the United States of America*, *107*, 9222–9227.